Available online at www.sciencedirect.com
SCIENCE DIRECT®
ELSEVIER
Solid State Communications 135 (2005) 340–344
solid state communications
www.elsevier.com/locate/ssc

# Band transitions in wurtzite GaN and InN determined by valence electron energy loss spectroscopy

P. Specht[a,b,*], J.C. Ho[a,b], X. Xu[a,b], R. Armitage[a,b], E.R. Weber[a,b], R. Erni[c,1], C. Kisielowski[d]

[a] *Materials Sciences Division, Lawrence Berkeley National Laboratory, University of California, One Cyclotron Road, Berkeley, CA 94720, USA*
[b] *Materials Science and Engineering Department, University of California, Berkeley, CA 94720, USA*
[c] *Department of Chemical Engineering and Materials Science, University of California, Davis, CA 95616, USA*
[d] *National Center for Electron Microscopy, LBNL, One Cyclotron Road, Berkeley, CA, USA*

Received 4 March 2005; accepted 21 April 2005 by F. Peeters
Available online 25 May 2005

## Abstract

Valence electron energy loss spectroscopy (VEELS) was applied to determine band transitions in wurtzite InN, deposited by molecular beam epitaxy on (0001) sapphire substrates or GaN buffer layers. The GaN buffer layer was used as VEELS reference. At room temperature a band transition for wurtzite InN was found at ($1.7 \pm 0.2$ eV) and for wurtzite GaN at ($3.3 \pm 0.2$ eV) that are ascribed to the fundamental bandgap. Additional band transitions could be identified at higher and lower energy losses. The latter may be related to transitions involving defect bands. In InN, neither oxygen related crystal phases nor indium metal clusters were observed in the areas of the epilayers investigated by VEELS. Consequently, the obtained results mainly describe the properties of the InN host crystal.
© 2005 Elsevier Ltd. All rights reserved.

*PACS:* 71.20.Nr; 71.55.Eq

*Keywords:* A. Indium-nitride; D. Bandgap; E. VEELS

The fundamental bandgap of InN is a topic of great controversy at present. Various research groups (see for example [1,2]) pursue the 'low-bandgap' theory which positions the fundamental bandgap of InN around 0.7 eV while others [3,4] repeatedly found evidence for a higher bandgap around 1.9 eV. In nano-structured and/or high indium-rich materials [5], a bandgap between 1.1 and 1.5 eV was also proposed. Many of these studies relate to optical measurements that require modeling for the interpretation of the data, which can be challenging in cases, where a large point defect concentration is involved. For example, it was found in low-temperature grown GaAs (LT-GaAs), which contains high concentrations of arsenic antisite defects that the optical properties can be dominated by the crystal defects rather than the host material itself. In particular, photoluminescence spectra (see for example [6]) and optical absorption spectra (see for example [7]) can be dominated by defect bands. Both optical methods were repeatedly used to determine the fundamental bandgap of InN (for example [1,2]) which also contains point defects in large concentrations and additionally a large concentration of dislocations. A correlation of InN absorption spectra to the

* Corresponding author. Address: Materials Sciences Division, Lawrence Berkeley National Laboratory, University of California, One Cyclotron Road, Berkeley, CA 94720, USA. Tel.: +1 510 495 2934; fax: +1 510 486 4995.
*E-mail address:* specht@socrates.berkeley.edu (P. Specht).
[1] Present address: FEI Electron Optics, P.O. Box 80066, 5600 KA Eindhoven, The Netherlands.

0038-1098/$ - see front matter © 2005 Elsevier Ltd. All rights reserved.
doi:10.1016/j.ssc.2005.04.041

epilayers' carrier concentration was made by applying the Moss–Burstein theory to InN [8]. However, this description is incomplete at best as it does not take into account the surface or interface conductivity [9] of the InN epilayers. This is large—and may be dominant—in most InN epilayers with free electron concentrations of nominally $10^{16}\,cm^{-3}$ [10] or higher. Consequently, the bandgap discussion should benefit when different methods are applied to determine the fundamental bandgap of InN. In this paper, we choose to identify for the first time band transitions in InN by valence electron energy loss spectroscopy (VEELS). Hexagonal GaN was used as a standard to evaluate the accuracy of the measured band transitions.

InN epilayers were deposited directly onto pre-nitridated (0001) sapphire substrates, on metal-organic chemical vapor deposition (MOCVD) grown GaN or molecular beam epitaxy (MBE) grown GaN buffer layers, both first deposited on (0001) sapphire. Typical InN epilayer thicknesses were 800–1000 nm, and the deposition was done under In-rich conditions. The oxygen concentration of the investigated epilayers varied between $10^{18}$ and $10^{20}\,cm^{-3}$, determined by SIMS analysis [11], and had no influence on the results reported here. The free electron concentration of the epilayers as determined by Hall measurements in Van der Pauw geometry ranged between $8\times10^{18}$ and $2\times10^{20}\,cm^{-3}$, the respective absorption spectra of the epilayers correlate with the Burstein–Moss theory [8], bandgap energies calculated according to [8] are between 0.8 and 1.3 eV. Further details of the epilayer growth are described elsewhere [11].

TEM samples were prepared in cross-sectional geometry by Ar ion milling and—in some cases—a final etching step to minimize surface roughness [12]. The VEELS measurements were performed with a monochromated FEI Tecnai $G^2$ STEM/TEM, which allows for a beam size of approximately 1 nm with an energy resolution in the spectra of better than 200 meV in scanning transmission mode. First, GaN buffer layers were investigated to provide a reference signal that was extensively studied before (see for example [13,14]). VEELS measurements were accompanied by high-resolution transmission electron microscopy to determine the crystal structure of the epilayers and to identify other phases if present. VEELS spectra were only taken from areas identified as pure wurtzite InN or wurtzite GaN with no other crystal phases present.

Fig. 1 shows a typical low energy VEELS spectrum of a GaN buffer layer. The top inset displays the recorded signal while the main figure shows the spectrum with contributions of the zero loss being removed. The bottom inset of Fig. 1 is the first derivative of the processed signal that can be described by a superposition of Lorentz functions (smooth curve in bottom inset) within the experimental noise. This fitting procedure was utilized to characterize the various band transitions by their inflection points as suggested previously by Lazar et al. [13]. We prefer this description over the commonly used bandgap determination by a power

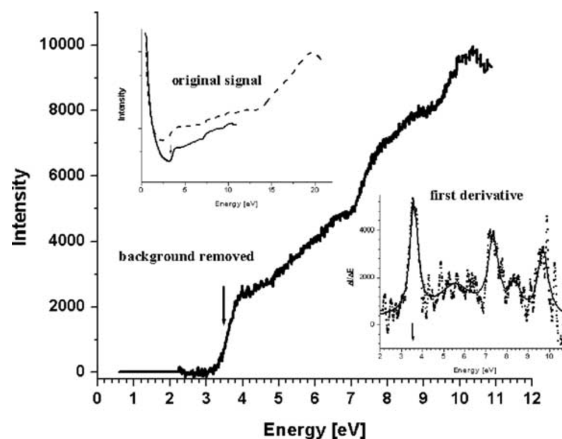


Fig. 1. Electron energy loss spectra showing band transitions in GaN, top inset: original spectrum with zero loss peak, bottom inset: first derivative of spectra after background subtraction, displays the point of deflection of various transitions.

law $(E-E_g)^{0.5}$ [14] that is more suitable if no signal overlap occurs. However, the power law fit describes the onset of the band transition (energy at zero intensity) and, therefore, the fundamental bandgap while the point of inflection method systematically results in higher energies. A comparison of both methods reveals that the energies extracted for GaN are at ($3.5\pm0.1$ eV) and ($3.3\pm0.1$ eV) for inflection point (IP) and power law (PL) methods, respectively. Using the FWHM of the respective peaks in the derivative plot one can link both methods and determine the bandgap $E_G$ to

$$E_G = E_{PL} \approx E_{IP} - 0.5\times\mathrm{FWHM} \quad (1)$$

Values given in this paper include this correction. A bandgap energy of 3.3 eV for GaN fits well with the accepted literature values for GaN at room temperature (3.4 eV). Considering an elevated temperature is a reasonable assumption as the investigated material under the electron beam is likely slightly heated. In the following, room temperature conditions are assumed.

In some InN epilayers which were deposited on top of MOVPE grown GaN buffer layers, wurtzite and zincblende InN grains coexist. In thin TEM sample areas, those phases can be investigated separately. Power spectra taken from local image areas allow for their identification. The analysis of zincblende InN will be published elsewhere. Local VEELS measurements were performed after identification of the respective phase of the grain, a typical spectrum for wurtzite InN is shown in Fig. 2. It is clearly visible that the first strong peak in the derivative energy spectra is located at an energy of about 1.9 eV. A multitude of different spectra were taken from various areas of three different InN epilayers, all were found to be similar to the one shown in Fig. 2. The corrected (room temperature) bandgap energy is ($1.7\pm0.2$ eV) for wurtzite InN. In rare cases and only for the InN epilayers with very high oxygen concentrations

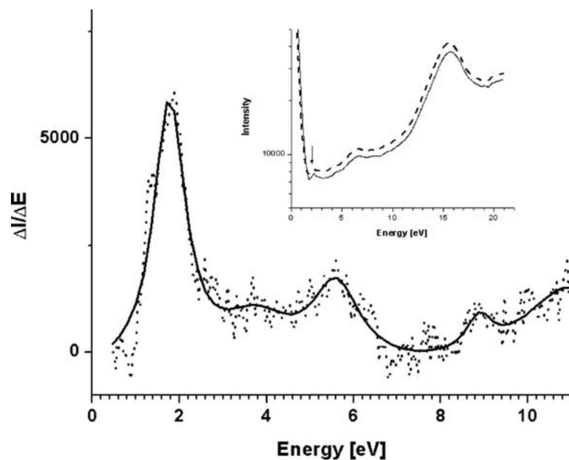


Fig. 2. First derivative of the electron energy loss spectrum of wurtzite InN, the inset shows the original spectrum.

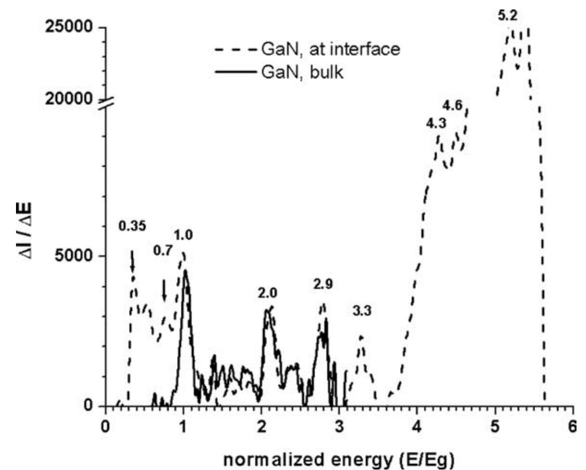


Fig. 3. Energy normalized VEELS first derivative spectra ($\Delta I/\Delta E$) of wurtzite GaN: $E_{\text{norm}}$ (GaN) = $E$/3.5 eV.

($\approx 10^{20}$ cm$^{-3}$) small indium oxide precipitates were observed, and indium metal clusters were never found. The areas investigated with VEELS did not contain any precipitates.

Part of the study of the electronic structure of InN via low loss VEELS is the identification of the plasmon peak. It's energy is given by [14]:

$$E_p(n) = \hbar\omega_p = \hbar\sqrt{\frac{ne^2}{\varepsilon_0 m}} \quad (2)$$

where $n$ is the number of valence electrons per unit volume and $m$ is the effective mass of the electrons. Taking $m_0$ as the effective electron mass the plasmon peak, now only dependent on the lattice constants of the epilayers, was calculated to be 22.3 eV for GaN and 19.2 eV for InN [14]. The experimental value for GaN, however, was determined to be (19.6 ± 0.1 eV) [14] which corresponds well with the value of (19.5 ± 0.1 eV) observed in this study, Fig. 1. The plasmon peak of InN determined here is (15.7 ± 0.1 eV) and does not vary for different samples. The variation in lattice constants, as measured for the various investigated samples [11], will only lead to a shift of the plasmon peak of ± 0.1 eV which is of the order of the measurement error. The observation of a constant plasmon peak position for different InN samples is, therefore, to be expected. Indium-oxide or oxy-nitride phases, however, should result in a different plasmon peak position. This result again documents that the material investigated here is pure InN.

Band transitions in GaN were found to differ when areas close to a GaN/InN interface were probed in an annealed heterostructure. Chemical analysis (EDS) does not show any indication of Ga-In interdiffusion in the area investigated and the plasmon peak of the VEELS spectra is still at 19.5 eV. However, additional transitions below bandgap appear, as can be seen in Fig. 3. In this figure, the energy for the band transitions in the d$I$/d$E$ plots is normalized to the 3.5 eV point of inflection. Below bandgap transitions in GaN may be assigned to defect transitions. The energy level at 0.7 in Fig. 3, for example, which translates to 2.45 eV, matches with the energy for the in GaN prominent yellow luminescence which is often correlated with the gallium vacancy [15], an intrinsic defect found in most n-type and semi-insulating GaN epilayers. Consequently, the annealed GaN epilayer in this study seems to contain defects, which are inhomogeneously distributed and accumulated at the interface to the InN. To our knowledge this is the first time defect transitions are observed by VEELS.

The band transitions in wurtzite GaN and InN are compared using the respective fundamental bandgap energy for normalization as a first approximation. From Fig. 3 seven band transitions were taken and the corresponding energy levels for wurtzite InN calculated using 1.9 eV as the norm. These resulting transitions are indicated as arrows in Fig. 4 which shows selected d$I$/d$E$ plots for three different InN epilayers. The epilayers' free electron concentration is given in Fig. 4 as well demonstrating that very different InN materials show quite similar band transitions and especially the same first transition which is suggested to be the fundamental bandgap. Table 1 shows the respective energy values of the band transitions (which are corrected as described in Eq. (1)) and their assignment to specific transitions using prior published data for comparison [3,16]. The error in the energy values are ± 0.2 eV for all GaN peaks and the below bandgap and bandgap peak in InN. For higher band transitions in InN the experimental error is higher (broader peaks, small shifts from one spectra to next) with values between ± 0.3 and ± 0.6 eV. Higher band transitions agree reasonably well with earlier published data. However, it is surprising that the 'down-scaling' from GaN band transitions also agrees quite well as this seems to indicate that GaN and InN exhibit similar band features. Again, in InN spectra energy peaks appear below the strong

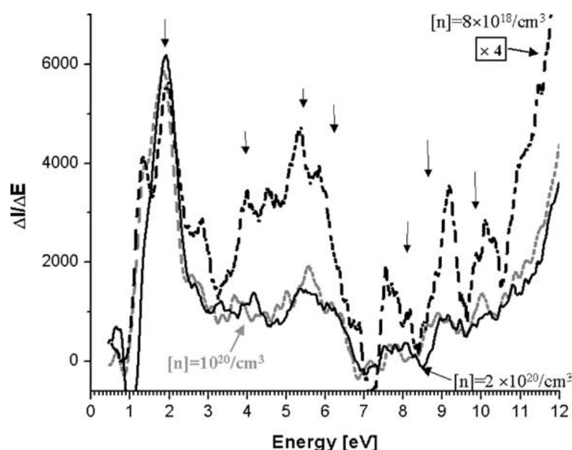


Fig. 4. First derivative spectra ($\Delta I/\Delta E$) of various wurtzite InN samples; the free electron concentration is given to distinguish the epilayers; arrows show estimated energy transitions, for details see text.

1.9 eV point of inflection which may also be correlated to defect (band) transitions. As InN is still a very defective material the appearance of defect related transitions is expected.

The assignment of specific band transitions to the observed VEELS edges is difficult because of the presence of various calculated band structure models but also due to expected energy values being similar for different band transitions. Table 1 shows an agreement of the here obtained experimental data with a selectively chosen literature data set and, therefore, is meant as one possible interpretation. In addition, the signal-to-noise ratio of the VEELS spectra for InN is still large, likely due to the high concentration of defects present in the investigated epilayers. The latter difficulty could be overcome by recording a large number of VEELS spectra and only the dominant features which were found frequently are discussed here.

For the fundamental bandgap and the plasmon peak of InN, however, the evaluation is more straight-forward as those energy losses are both pronounced, the lowest energy transition is consistent in all spectra of wurtzite InN and the plasmon peak position is mainly dependent on the crystalline structure and the lattice parameters of the material, both of which are known (for lattice parameter determination see Ref. [11]). These investigations clarify that a band transition around 1.7 eV does exist in wurtzite InN although in this energy range optical material responses are hardly ever found. If the 1.7 eV band transition is indeed the fundamental bandgap in InN at room temperature it is concluded that defect bands, grain boundaries, dislocations and/or the very conductive surface are contributing to the lower energy optical responses in InN. The identification of the various defects in InN will be subject of future investigations.

In conclusion, band transitions in wurtzite GaN and InN were observed utilizing low loss VEELS with a monochromated electron beam. The dominant energy peaks in the VEELS spectra have been preliminarily assigned to band transitions using Refs. [3,16] for comparison. Clearly, a dominant energy transition is observed for wurtzite InN at approximately ($1.7\pm0.2$ eV). This transition is assumed to be the fundamental bandgap of wurtzite InN at approximately 300 K. The plasmon peak energy for InN was determined ($15.7\pm0.1$ eV). For the first time, below bandgap energy losses were observed in GaN, which may be related to deep level defect band transitions. Similar transitions were also found in InN.

## Acknowledgements

This work was financially supported by the Air Force Office of Scientific Research under contract no. FA9550-04-1-0408 and by the Director, Office of Science, Office of Basic Energy Sciences, of the US Department of Energy under contract no. DE-AC03-76SF00098. One of the authors (R.E.) was supported by the US Department of Energy under grant no. DE-FG02-03ER46057.

Table 1
Comparison of band transitions in wurtzite InN and GaN as found in the literature with experimental results from VEELS analysis, the experimental values were corrected according to Eq. (1)

| Exp. results, corrected energies: | | | Estimated: | Prior published for InN: | | |
|---|---|---|---|---|---|---|
| GaN (eV) | Normalized E (E/Eg_PI) | InN (eV) | InN (eV) | Tansley [3] (eV) | Fritsch [16] (eV) | Transitions |
| 3.3 | 1 | 1.7 | 1.7 | 2.1 | 2.6 | Γ_6V—Γ_1C |
| 6.8 | 2 | 3.6 | 3.6 | 5 | 5.2 | Γ_5V—Γ_3C |
| 10 | 2.9 | 5.3 | 5.3 | 5.4 | 7.3 | H_3V—H_3C |
| 11.4 | 3.3 | 5.9 | 6.1 | 7.3 | 6.7 | M_4V—M_3C |
| 14.9 | 4.3 | 7.6 | 8 | 7.3 | 8.1 | K_3V—K_2C |
| 15.9 | 4.6 | 8.9 | 8.5 | – | 8.6 | K_2V—K_2C |
| 18 | 5.2 | 9.9 | 9.7 | 8.8 | 10.2 | Γ_5V—Γ_6C |

## References


[1] V.Yu. Davydov, A.A. Klochikhin, R.P. Seisyan, V.V. Emtsev, et al., Phys. Status Solidi B 229 (2002) R1.

[2] J. Wu, W. Walukiewicz, K.M. Yu, J.W. Ager III, E.E. Haller, H. Lu, W.J. Schaff, Y. Saito, Y. Nanishi, Appl. Phys. Lett. 80 (2002) 3967.

[3] T.L. Tansley, C.P. Foley, J. Appl. Phys. 59 (1986) 3241.

[4] K.S.A. Butcher, M. Wintrebert-Fouquet, P.P.-T. Chen, H. Timmers, S.K. Shrestha, Mater. Sci. Semicond. Process. 6 (2003) 351.

[5] T. Inushima, V.V. Mamutin, V.A. Vekshin, S.V. Ivanov, T. Sakon, M. Motokawa, S. Ohoya, J. Cryst. Growth 227/228 (2001) 481; B. Maleyre, O. Briot, S. Ruffenach, J. Cryst. Growth 269 (2004) 15; T.V. Shubina, S.V. Ivanov, V.N. Jmerik, D.D. Solnyshkov, V.A. Vekshin, P.S. Kop'ev, A. Vasson, J. Leymarie, A. Kavokin, H. Amano, K. Shimono, A. Kasic, B. Monemar, Phys. Rev. Lett. 92 (2004) 117407.

[6] M. Tajima, H. Tanino, K. Ishida, in: H.J. von Bardeleben (Ed.), Proceedings of the 14th International Conference on Defects in Semiconductors, Trans Tech Publications Ltd, Aedermannsdorf, 1986, p. 1265.

[7] G.M. Martin, Appl. Phys. Lett. 39 (1981) 747.

[8] J. Wu, W. Walukiewicz, S.X. Li, R. Armitage, J.C. Ho, E.R. Weber, E.E. Haller, H. Lu, W.J. Schaff, A. Barcz, R. Jakiela, Appl. Phys. Lett. 84 (2004) 2805.

[9] H. Lu, W.J. Schaff, J. Hwang, H. Wu, G. Koley, L.F. Eastman, Appl. Phys. Lett. 79 (2001) 1489.

[10] H. Lu, W.J. Schaff, L.F. Eastman, C.F. Stutz, Appl. Phys. Lett. 82 (2003) 1736.

[11] P. Specht, R. Armitage, J. Ho, E. Gunawan, Q. Yang, X. Xu, C. Kisielowski, E.R. Weber, J. Cryst. Growth 269 (2004) 111.

[12] C. Kisielowski, Z. Liliental-Weber, S. Nakamura, Jpn. J. Appl. Phys. 36 (1997) 6932.

[13] S. Lazar, G.A. Botton, M.-Y. Wu, F.D. Tichelaar, H.W. Zandbergen, Ultramicroscopy 96 (2003) 535.

[14] V.J. Keast, A.J. Scott, M.J. Kappers, C.T. Foxon, C.J. Humphreys, Phys. Rev. B 66 (2002) 125319.

[15] K. Saarinen, P. Seppälä, J. Oila, P. Hautojärvi, C. Corbel, O. Briot, R.L. Aulombard, Appl. Phys. Lett. 73 (1998) 3253.

[16] D. Fritsch, H. Schmidt, M. Grundmann, Phys. Rev. B 67 (2003) 235205.